
Neutron Reflectometry

—
depth profile of the density in a layered Ni/Ti film

—
instrument: Morpheus

contact

	tel	mail
Jochen Stahn	056 310 2518	jochen.stahn@psi.ch
Thomas Geue	056 310 5988	thomas.geue@psi.ch
Panagiotis Korelis	056 310 5813	panagiotis.korelis@psi.ch

contents

1	introduction	2
2	theory	2
2.1	what is n for neutrons?	2
2.2	what is V_i for neutrons?	3
2.3	reflectance of an interface	3
2.4	the surface: Fresnel reflectivity	4
2.5	parallel interfaces, matrix formalism	6
2.6	some numbers	7
3	the experiment	8
3.1	the sample	8
3.2	measurement scheme, angle dispersive mode	9
3.3	alignment & measurements	9
3.4	data reduction	11
3.5	protocol	12

references

- [1] F. Ott: *Neutron scattering on magnetic surfaces*
Comptes Rendus Physique **8** 763 - 776 (2007).
DOI 10.1016/j.crhy.2007.09.002
- [2] J. Dailland, A. Gibaud, editors: *X-ray and Neutron Reflectivity*
Lect. Notes Phys. **770**, Springer, Berlin Heidelberg 2009.
DOI 10.1007/978-3-450-88588-7

1 introduction

Neutron reflectometry is a method to probe the laterally averaged nuclear and magnetic depth profiles close to a flat surface. More precisely this means: The reflectivity one gets from a surface of at least some mm^2 allows to validate (or falsify) a model of this surface describing its density and composition, and the in-plane magnetic induction. This method probes the density averaged laterally (parallel to the surface) over some $10\ \mu\text{m}$, but with a depth resolution of atomic dimensions. On the other side structures thicker than $0.5\ \mu\text{m}$ can hardly be resolved. The penetration depth of the neutron in reflectometry is some μm .

The principle of neutron reflectometry is quite similar to the partial reflection of optical light on a flat surface. This is illustrated on the example of the soap bubbles: A part of the light is reflected as can be seen by the mirror images of the surrounding. But depending on the angle of view, the image changes its colour. In addition the bubbles are partly transparent, allowing to see the bushes behind. By using a more precise set-up in terms of defined wavelength λ and direction of the light relative to the surface, one could extract the density of the soap film from the index of refraction n and its thickness from the colour of the reflected light.



The essential difference between light and neutrons is the nature of the probed potential. The interaction of light with matter is given by its polarisability, i.e. the mobility of electrons. Neutrons interact with the nuclei (the interaction is measured by the nuclear scattering length b) and with magnetic fields. As we will see later, the potential imposed upon the neutrons this way is rather small compared to their kinetic energy. As a consequence the index of refraction is almost 1. So in contrast to visible light with $n = 1 \dots 1.5$, the reflection effects for neutrons play on the very limited range of small angles of incidence, only.

The power of neutron reflectometry (NR) can be nicely demonstrated on the example of the depth-profile of the nuclear potential of a Ni/Ti multilayer. The scattering lengths of these materials are very different: $\bar{b}_{\text{Ni}} = 10.3 \cdot 10^{-5}\ \text{\AA}$ and $\bar{b}_{\text{Ti}} = -3.438 \cdot 10^{-5}\ \text{\AA}$.

In the following section an introduction into theory is given. The focus is on the dependence of n on the composition of the material. The effects of magnetic fields are mentioned for completeness. These are marked in blue. For the interpretation of the measurements the program code Parratt32 will be used. In the theory section the principle behind the algorithm is explained without going too much into details. A lot of these details can be found in Ott's paper [1], and especially in the book of Daillant and Gibaud [2].

Afterwards the experimental set-up and the sample are presented, followed by the description of the experiment and the data reduction.

2 theory

As we will see, there is no direct transformation from the finally measured intensity vs. momentum transfer back to the physical quantities we are interested in, i.e. the thicknesses and compositions of the films and eventually the depth profile of the magnetisation. In practise one has to simulate a reflectivity curve $R(q_z)$ and compare it to the measured and renormalised quantity $R(q_z) = I(q_z)/I_0$. The simulation is based on a model.

In the next subsections the index of refraction is reduced to some potential and finally to nuclear density and magnetic induction. In a next step the reflectance and transmittance of a single interface are deduced and finally a simplified method to calculate the reflectance of a series of parallel interfaces is given. The simplification is, to assume perfectly flat and sharp interfaces and no lateral inhomogeneity within the film.

2.1 what is n for neutrons?

The Schrödinger equation for a plane wave $\Phi = A e^{ik_i r}$ in a medium i is

$$\begin{aligned} \frac{\hbar^2}{2m} \frac{d}{dr} A e^{ik_i r} + (E - V_i) A e^{ik_i r} &= 0 \\ \frac{\hbar^2}{2m} (-k_i^2) e^{ik_i r} + (E - V_i) e^{ik_i r} &= 0 \end{aligned}$$

with the total energy E and the potential V_i of the medium i . This leads to the wavenumber

$$k_i^2 = (E - V_i) \frac{2m}{\hbar^2} \tag{1}$$

For the vacuum ($i := 0$) we define $V_0 = 0$. The index of refraction relates k_i to k_0 by

$$n_i^2 := \frac{k_i^2}{k_0^2} \quad (2)$$

$$= \frac{E - V_i}{E}$$

$$n_i = \sqrt{1 - V_i/E} \quad (3)$$

$$\approx 1 - V_i/2E \quad \text{for } V_i \ll E$$

$$:= 1 - \delta \quad (4)$$

As we will see in section 2.6, $|V_i| < 10^{-3}E$ so that the approximation made is well justified.

2.2 what is V_i for neutrons?

As the de Broglie wavelength of a neutron is orders of magnitude larger than the radius of a nucleus ($\lambda \gg r_{\text{nucleus } j}$) the interaction potential can be written in the form of a Fermi pseudo potential.

$$V_j^{\text{Fermi}}(\mathbf{r}) = b_j \frac{2\pi \hbar^2}{m} \delta(\mathbf{r})$$

b_j is the *scattering length* of the nucleus j , m is the neutron mass, and $\delta(\mathbf{y})$ is the Kronecker delta function. The integration over an ensemble i of nuclei then reduces to a summation:

$$\begin{aligned} V_i^n &= \frac{1}{\text{vol}} \int_{\text{vol}} V_j^{\text{Fermi}}(\mathbf{r}) \, d\mathbf{r} \\ &= \frac{2\pi \hbar^2}{m} \frac{1}{\text{vol}} \sum_j b_j \\ &:= \frac{2\pi \hbar^2}{m} \rho_i^b \end{aligned} \quad (5)$$

So the V is reduced to a *nuclear scattering length density* ρ^b . If in addition a magnetic induction \mathbf{B} is present, the neutron experiences also a magnetic potential due to its magnetic moment μ_n :

$$V^m = \mu_n \mathbf{B} \quad (6)$$

$$:= \frac{2\pi \hbar^2}{m} \rho^m \quad (7)$$

Depending on the relative orientation of μ_n and \mathbf{B} one gets $V^m = \pm \mu_n B$. The introduction of a *magnetic scattering length density* ρ^m sometimes simplifies the calculation. The interpretation of ρ^m in terms of *magnetic moment per atom* is dangerous because \mathbf{B} can not be regarded as a sum over δ -functions.

Eqn.3 tells that n_i depends finally on the averaged nuclear scattering length density ρ^b , and on B and the *polarisation* of the neutron. With the energy of the free neutron $E = \hbar^2 k_0^2 / 2m = 4\pi^2 \hbar^2 / 2m \lambda^2$ eqn.4 can be written as

$$n_i \approx 1 - \frac{\lambda^2}{2\pi} (\rho_i^b + \rho_i^m) \quad (8)$$

2.3 reflectance of an interface

The reflectivity of a sample is defined by

$$R = \left| \frac{A_0^\uparrow}{A_0^\downarrow} \right|^2 \quad (9)$$

where A_0^\downarrow is the amplitude of the incoming (from vacuum) plane wave and A_0^\uparrow is the amplitude of the reflected wave. The intensity is proportional to the amplitude squared. Fig.1 illustrates the beam paths of a plane wave partly reflected at a single interface.

In the following the reflectance and transmittance of a single interface between the materials i and $i+1$ is deduced. Exactly at the interface (at $\mathbf{r} = \mathbf{r}_{i,i+1}$) the continuity conditions

$$\begin{aligned} \Psi_i(\mathbf{r}_{i,i+1}) &= \Psi_{i+1}(\mathbf{r}_{i,i+1}) \\ \frac{d}{d\mathbf{r}} \Psi_i(\mathbf{r}_{i,i+1}) &= \frac{d}{d\mathbf{r}} \Psi_{i+1}(\mathbf{r}_{i,i+1}) \end{aligned} \quad (10)$$

apply for all $\mathbf{r}_{i,i+1}$ where Ψ_i is the wavefunction in layer i . This means that the x and y components (in-plane) of Ψ are not affected by the change of n . So only the z -component has to be regarded. This can be written as

$$\Psi_{z,i} = A_i^\uparrow e^{ik_{z,i}z} + A_i^\downarrow e^{-ik_{z,i}z} \quad (11)$$

in medium i . Thus with eqns. 10 one gets

$$\begin{aligned} \Psi_{z,i} &= \Psi_{z,i+1} \\ A_i^\uparrow e^{ik_{z,i}z} + A_i^\downarrow e^{-ik_{z,i}z} &= A_{i+1}^\uparrow e^{ik_{z,i+1}z} + A_{i+1}^\downarrow e^{-ik_{z,i+1}z} \end{aligned} \quad (12)$$

and

$$\begin{aligned} \frac{d}{dz}\Psi_{z,i} &= \frac{d}{dz}\Psi_{z,i+1} \\ ik_{z,i}A_i^\uparrow e^{ik_{z,i}z} - ik_{z,i}A_i^\downarrow e^{-ik_{z,i}z} &= ik_{z,i+1}A_{i+1}^\uparrow e^{ik_{z,i+1}z} - ik_{z,i+1}A_{i+1}^\downarrow e^{-ik_{z,i+1}z} \end{aligned} \quad (13)$$

The ratio of the amplitudes of the up- and down-travelling wave components in material i are called reflectance of the interface $i, i + 1$ if the up-travelling wave is formed only by reflection of the down-travelling wave on that interface.

$$r_{i,i+1} = \frac{A_i^\uparrow}{A_i^\downarrow} \quad (14)$$

In analogy the transmittance is defined by

$$t_{i,i+1} = \frac{A_{i+1}^\downarrow}{A_i^\downarrow} \quad (15)$$

These quantities can be calculated using eqns. 12 and 13. This is a lengthy exercise in boring book keeping. The result can be given as a function of k_i and k_{i+1} or by using $k_{z,i} = k_i \sin \omega_i$ and $k_i = n_i k_0$ as a function of the angles ω_i under which \mathbf{k}_i hits the interface.

$$\begin{aligned} r_{i,i+1} &= \frac{k_{z,i} - k_{z,i+1}}{k_{z,i} + k_{z,i+1}} \\ &= \frac{n_i \sin \omega_i - n_{i+1} \sin \omega_{i+1}}{n_i \sin \omega_i + n_{i+1} \sin \omega_{i+1}} \end{aligned} \quad (16)$$

$$\begin{aligned} t_{i,i+1} &= \frac{2k_{z,i}}{k_{z,i} + k_{z,i+1}} \\ &= \frac{2n_i \sin \omega_i}{n_i \sin \omega_i + n_{i+1} \sin \omega_{i+1}} \end{aligned} \quad (17)$$

The angles ω_i and ω_{i+1} are related by Snell's law:

$$\frac{\cos \omega_i}{\cos \omega_{i+1}} = \frac{n_{i+1}}{n_i} \quad (18)$$

2.4 the surface: Fresnel reflectivity

In the case of a single interface vacuum/material eqn. 16 can be rewritten

$$r_{0,1} = \frac{\sin \omega - n \sin \omega_1}{\sin \omega + n \sin \omega_1} \quad (19)$$

$$= \frac{\sin \omega - n \sqrt{1 - \cos^2 \omega / n^2}}{\sin \omega + n \sqrt{1 - \cos^2 \omega / n^2}} \quad (20)$$

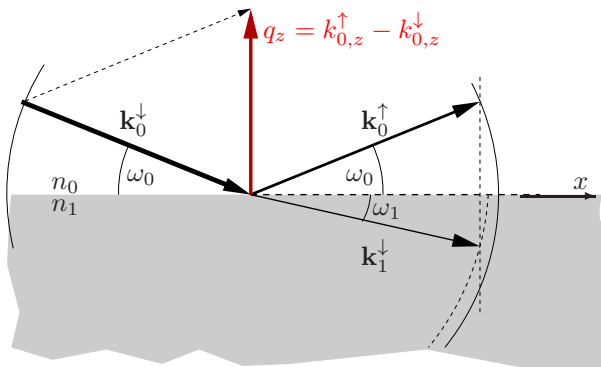


Figure 1: Sketch to illustrate the beam paths in a reflectivity measurement. Only the scattering plane (x/z -plane) is shown. \mathbf{k}_0^\downarrow is the wavevector of the incoming beam, \mathbf{k}_0^\uparrow is the reflected and \mathbf{k}_1^\downarrow the transmitted beam. ω_i gives the angle between \mathbf{k}_i and \mathbf{x} ; and q_z represents the momentum transfer normal to the surface.

For $\cos \omega = n$ this leads to $r_{0,1} = 1$, i.e. to total external reflection. Thus one can define the *critical angle of total reflection* ω^c by

$$\begin{aligned} \cos \omega^c &:= n \\ 1 - \frac{\omega^{c2}}{2!} + \frac{\omega^{c4}}{4!} - \dots &= 1 - \delta \end{aligned} \quad (21)$$

$$\begin{aligned} \frac{\omega^{c2}}{2} &\approx \frac{\lambda^2}{2\pi} (\rho^b + \rho^m) \\ \omega^c &\approx \sqrt{\frac{\rho^b + \rho^m}{\pi}} \lambda \end{aligned} \quad (22)$$

The cos function was rewritten as a power series and cut after the quadratic term; δ was substituted using eqns. 3. To get rid of the experimental parameters λ and ω one often uses the (wavenumber of the) momentum transfer normal to the surface

$$\begin{aligned} q_z &= -2k_0 \\ &= \frac{4\pi \sin \omega}{\lambda} \end{aligned} \quad (23)$$

For small ω one can use $\sin \omega \approx \omega$ and the resulting *critical momentum transfer* is

$$q^c = 4 \sqrt{\pi(\rho^b + \rho^m)} \quad (24)$$

and the reflectance of a single interface can be written as

$$\begin{aligned} r_{0,1} &= \frac{1 - \sqrt{1 - (q^c/q_z)^2}}{1 + \sqrt{1 - (q^c/q_z)^2}} \quad \forall q_z \geq q^c \\ &= 1 \quad \forall q_z < q^c \end{aligned} \quad (25)$$

The reflectivity in this case is called *Fresnel reflectivity*:

$$R^{\text{Fresnel}}(q_z) = |r_{0,1}(q_z)|^2 \quad (26)$$

Figure 2 shows $R^{\text{Fresnel}}(q_z)$ together with the function $(4q_z/q^c)^{-4}$ to display the strong decrease of $R(q_z)$ with increasing q_z . In cases where the assumptions of ideally flat and sharp interfaces and of a homogeneous material do not apply, the intensity decreases even more rapidly. The reason is that also scattering in other directions occurs, reducing the effective intensity of the incoming wave.

From eqn. 24 one can see that $q^{c2} \propto \rho^b + \rho^m$. This can be used to extract ρ^b and finally b of a non-magnetic material and to measure the mean magnetisation of the surface area: By using neutrons polarised parallel and antiparallel to B one gets 2 critical edges at $q^{c,\text{up}2} \propto \rho^b + |\rho^m|$ and at $q^{c,\text{down}2} \propto \rho^b - |\rho^m|$, respectively. Thus $\rho^m \propto q^{c,\text{up}2} - q^{c,\text{down}2}$.

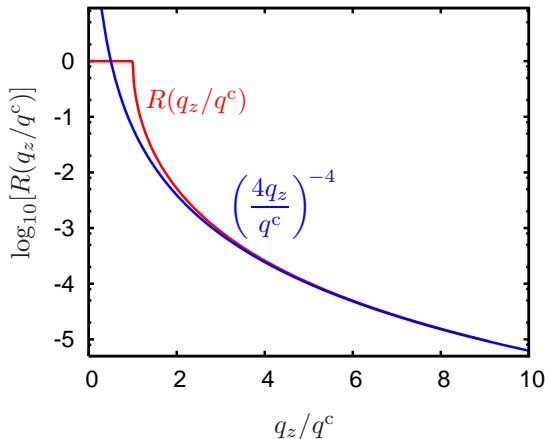


Figure 2: (red curve) Simulated reflectivity $R(q_z)$ of a single interface (vacuum / material 1). The q_z axis is renormalised to the critical momentum transfer q^c . To illustrate the strong decay of $R(q_z)$ above q^c also the asymptote is shown in blue curve.

2.5 parallel interfaces, matrix formalism

Now we will have a look at the situation with several parallel interfaces. The wave fields formed in a multilayer are quite complex and one finally measures an outgoing wave which is formed by interference defined by all layers. I.e. by their n_i , their thicknesses d_i and their order. A rather simple approach to calculate $R(q_z)$ for a given multilayer is the *matrix formalism*. Still assuming homogeneous layers and sharp interfaces this leads to a transparent description.

The wavefield outside the sample but just at the interface is

$$\Psi_0(z=0) = \begin{pmatrix} A_0^\uparrow \\ A_0^\downarrow \end{pmatrix}$$

where the phase factor vanished because of the free choice of the origin, i.e. $z=0$ at the interface. $\Psi_0(z=0)$ is related to the wavefield inside the first layer, also at the interface, by

$$\Psi_0(z=0) = \begin{pmatrix} 1/t_{0,1} & r_{0,1}/t_{0,1} \\ r_{0,1}/t_{0,1} & 1/t_{0,1} \end{pmatrix} \begin{pmatrix} A_1^\uparrow \\ A_1^\downarrow \end{pmatrix}$$

where the continuity condition (equations 10) has been used. The interface matrix \mathbf{I} contains elements made up from the reflectance and transmittance of the interface. These in turn depend on q_z . If we knew A_1^\uparrow and A_1^\downarrow we were able to calculate A_0^\uparrow . We do not know these quantities but we can relate the unknown situation at $z=0$ to the next interface at $z=-d_1$:

$$\Psi_0(z=0) = \mathbf{I}_{0,1} \begin{pmatrix} e^{ik_{z,1}d_1} & 0 \\ 0 & e^{-ik_{z,1}d_1} \end{pmatrix} \begin{pmatrix} A_1^\uparrow e^{-ik_{z,1}d_1} \\ A_1^\downarrow e^{ik_{z,1}d_1} \end{pmatrix}$$

and obtain a matrix \mathbf{T}_1 giving phase factors. Now we repeat the procedure from interface 0,1 and so on:

$$\begin{aligned} \Psi_0(z=0) &= \mathbf{I}_{0,1} \mathbf{T}_1 \begin{pmatrix} 1/t_{1,2} & r_{1,2}/t_{1,2} \\ r_{1,2}/t_{1,2} & 1/t_{1,2} \end{pmatrix} \begin{pmatrix} A_2^\uparrow e^{-ik_{z,1}d_1} \\ A_2^\downarrow e^{ik_{z,1}d_1} \end{pmatrix} \\ &= \mathbf{I}_{0,1} \mathbf{T}_1 \mathbf{I}_{1,2} \begin{pmatrix} e^{ik_{z,2}d_2} & 0 \\ 0 & e^{-ik_{z,2}d_2} \end{pmatrix} \begin{pmatrix} A_2^\uparrow e^{-ik_{z,2}(d_1+d_2)} \\ A_2^\downarrow e^{ik_{z,2}(d_1+d_2)} \end{pmatrix} \\ &\vdots \\ &:= \mathbf{M} \begin{pmatrix} A_{\text{substr}}^\uparrow e^{-ik_{z,\text{substr}} \sum_i d_i} \\ A_{\text{substr}}^\downarrow e^{ik_{z,\text{substr}} \sum_i d_i} \end{pmatrix} \end{aligned} \quad (27)$$

We end up with a matrix \mathbf{M} which relates the wave outside the sample to the situation inside the substrate, just below the last interface. Now we can assume that there is no up-travelling wave in the substrate, so $A_{\text{substr}}^\uparrow = 0$, and

$$\Psi_0(z=0) = \mathbf{M} \begin{pmatrix} 0 \\ A_{\text{substr}}^\downarrow e^{ik_{z,\text{substr}} \sum_i d_i} \end{pmatrix} \quad (28)$$

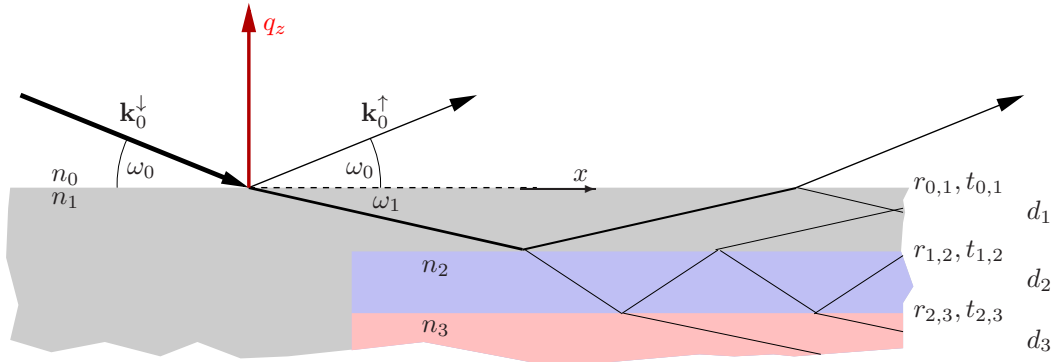


Figure 3: Sketch to illustrate the beam paths in a sample with several parallel interfaces. The nomenclature is the same as in Fig. 1. The sample is characterised by the index of refraction n_i and the thickness d_i of the layers i .

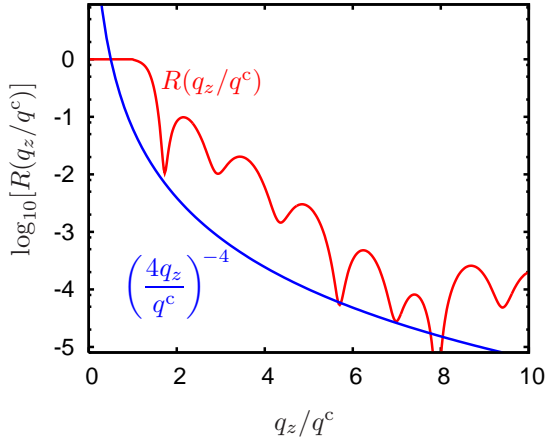


Figure 4: Simulated reflectivity curve $R(q_z)$ of a sample with several parallel interfaces. The q_z axis is renormalised to the critical momentum transfer q^c of the substrate (the lowest interface). The modulation of $R(q_z)$ above q^c is the result of the interferences of the waves reflected at the various interfaces.

And finally we are not interested in A_0^\uparrow and A_0^\downarrow but in the reflectance of the complete multilayer:

$$\begin{aligned}
 r(q_z) &= \frac{A_0^\uparrow}{A_0^\downarrow} \\
 &= \frac{M_{12} A_{\text{substr}}^\downarrow e^{ik_{z,\text{substr}} \sum_i d_i}}{M_{22} A_{\text{substr}}^\downarrow e^{ik_{z,\text{substr}} \sum_i d_i}} \\
 &= \frac{M_{12}}{M_{22}}
 \end{aligned} \tag{29}$$

or better in its reflectivity

$$R(q_z) = \left| \frac{M_{12}(q_z)}{M_{22}(q_z)} \right|^2 \tag{30}$$

Now we have a simple but time-consuming method to calculate $R(q_z)$ starting from a model giving $\rho^b(z)$ and thus n_i and d_i . The calculation must be done for each value of q_z individually.

To compare the simulated reflectivity with measured curves one has in general to take additional effects into account. E.g.

- non-sharp interfaces
- under- or over-illumination of the sample
- resolution of the set-up resulting in $\Delta\omega$, $\Delta\lambda$

More sophisticated approaches take laterally inhomogeneous layers into account. The problem there is the length-scale of the inhomogeneity: on long distances one gets a sum of specularly reflected beams. On the short scale one averages over the inhomogeneity and one is back at the presented algorithm. In between one has partial interference. We leave this topic to the real experts and concentrate on what we need for the planned experiment.

2.6 some numbers

In the theory part some approximations were made, essentially based on the statement that $V_i \ll E \quad \forall i$. Using eqn. 4 and some extreme input values (for cold neutrons, i.e. $\lambda > 2 \text{ \AA}$) one can estimate the validity of this statement. The element with the largest scattering length density in Ni with $\bar{b} = 10.3 \cdot 10^{-5} \text{ \AA}$ and a resulting $\rho^b = 9.41 \cdot 10^{-6} \text{ \AA}^{-2}$.

$$\begin{aligned}
 \delta^n &= \frac{V^n}{2E} = \frac{\lambda^2}{2} \rho^b \\
 &< 2 \cdot 10^{-3} \quad \text{for } \lambda = 20 \text{ \AA}
 \end{aligned}$$

A high magnetic induction with $B = 10 \text{ T}$ leads to

$$\begin{aligned}
 \delta^m &= \frac{V^m}{2E} = \frac{\mu_n B}{2\pi^2 \hbar^2 / m \lambda^2} \\
 &< 2 \cdot 10^{-3} \quad \text{for } \lambda = 20 \text{ \AA}
 \end{aligned}$$

with $\mu_n = -0,96623641(23) \cdot 10^{-26} \text{ J/T}$ and $m = 1,674927211(84) \cdot 10^{-27} \text{ kg}$.

3 the experiment

3.1 the sample

The sample is a multilayer of Ni and Ti on glass. This means that on a flat and clean glass (SiO_2) substrate an alternating stack of Ni and Ti layers are deposited. The thicknesses of the layers are constant and of the order of 100 Å to 200 Å. The periodic nature of the multilayer leads to conditions for destructive (minima) and constructive (main maxima) interferences, similar to diffraction or to the scattering of light on an optical grid.

Table 1 contains the parameters to be used for the calculation of $\rho^b(z)$.

element / material	\bar{b} 10^{-5} Å	ρ cm^3	M g/mol
Ni	10.3	8.91	58.69
Ti	-3.438	4.51	47.88
Si	4.1491	2.32	28.09
O	5.803	-	16.00
SiO_2	-	2.13	-

Table 1: Physical parameters of the materials and elements involved. \bar{b} is the scattering length, averaged over the natural isotope concentration. ρ is the mass density and M the atomic weight.

$$1 \text{ mol} = 6.022\,141\,79(30) \cdot 10^{23}$$

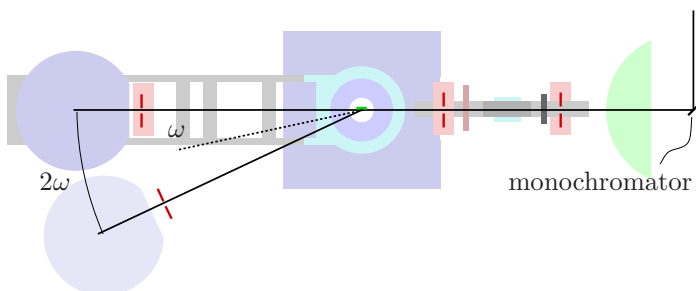
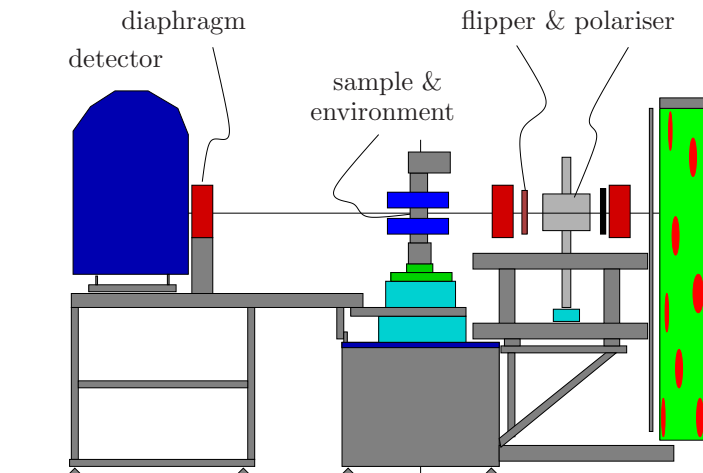
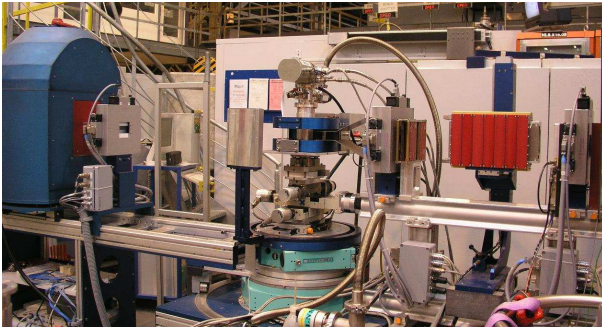


Figure 5: The angle dispersive neutron reflectometer Morpheus at SINQ, PSI. The photo shows a possible configuration of Morpheus allowing for polarised neutron reflectometry measurements.

The essential elements are reproduced in the sketch below. They are from right to left (following the beam)

- The monochromator: a graphite single crystal which extracts a beam with $\lambda = 5$ Å from the white beam.

- The polariser: a multilayer of Fe and Si, reflecting spin-up neutrons, only. The transmitted beam is spin-down polarised.

- The flipper: to flip the spin state from down to up if needed.

- The sample environment: equipment to hold and adjust the sample, allowing for ω rotation; And equipment to define the conditions on and around the sample, here a Helmholtz coil to apply a magnetic field and a cooling device. For non-polarised measurements an Euler cradle will be installed to allow for a precise alignment of the sample

- The detector: a ^3He filled wire detector.

- Diaphragms are installed before and after the sample to define $\Delta\omega$ and thus the resolution, and to reduce the background in the detector.

The lower sketch shows Morpheus from top to illustrate the rotations of the sample and the detector.

3.2 measurement scheme, angle dispersive mode

We will have to determine $R(q_z)$. But we measure some intensity as a function of some variable(s). For the intensities its quite simple: $R = I^\uparrow/I^\downarrow$, where I^\downarrow is the total intensity hitting the sample (which might be different from the intensity of the incoming beam). And I^\uparrow is the intensity of the reflected beam. For the variables: Eqn.23 leaves us 2 choices to scan q_z : One can vary the wavelength λ of the incoming neutrons, keeping ω fixed (energy dispersive set-up); Or one can fix λ and vary ω (angle dispersive set-up).

The energy dispersive mode is often used when liquid samples are involved. In most cases it is not possible to tilt the neutron source to change ω . And it is even more difficult to tilt a liquid surface. An example for an experiment using the energy dispersive mode is the reflectometer Amor at SINQ, PSI.

Most reflectometers operate in the angle dispersive mode. Fig. 6 illustrates the measurement scheme: The incoming beam hits the sample at a small angle ω . This is varied by tilting the sample with respect to the beam. The detector has to be rotated around the same axis, but by 2ω . The general instrument lay-out to allow for these movements is shown in Fig. 5 on the example of the reflectometer Morpheus, also at PSI.

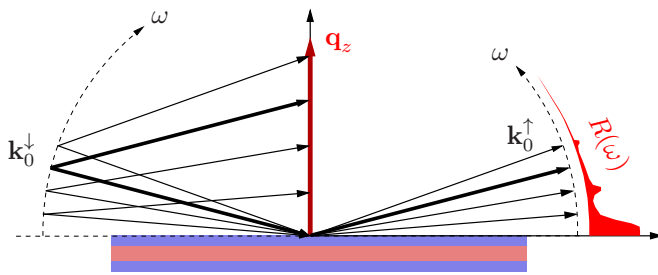


Figure 6: Measurement scheme of the angle dispersive reflectometry. The incoming beam has a constant λ , but the orientation relative to the sample surface is varied. The lower part of the sketch is the real world cartoon of the sample. Above its surface the momentum space representation of the beams is given.

3.3 alignment & measurements

The first step will be to set-up the NR option on the instrument Morpheus and to align it without the sample. This will be done by the adviser.

The next step will be to mount and align the sample. The beam width will be around 1 mm, the ω range to be covered is $0 < \omega < 3^\circ$. This means that the alignment has to be very accurate.

1. rough alignment with a laser: A laser is installed behind the monochromator and allows to position the sample by eye at the correct height (z of the instrument) and in the direction normal to the beam (y of the instrument). The latter movement is motorised and has the name **sty**

> dr sty <value> drive sample translation in y-direction to value

Also the sample surface can be roughly aligned parallel to the beam via the rotation **som**. After alignment the scale for ω should be reset by

> sp som 0 set position of sample omega to be 0

2. The substrate of the sample is glass containing some Boron. B is a neutron absorber, thus the substrate is not transparent. This fact can be used to improve the alignment: The detector is positioned at $2\omega = 0^\circ$ with the command

> dr stt 0 drive sample two theta to 0

and the sample is scanned normal to the beam

> sscan sty -2 2 41 2000 step-scan of sty from -2° to 2°
with 41 points and 2000 counts in the monitor

If the rough alignment was not too bad, one should see a step profile: full intensity when the sample is not in the beam, a strong decay (depending on the width of the beam), and low intensity if the sample shades the beam. The sample is to be moved to the step by

> dr sty <value> drive sty to value

3. If ω was already correct a scan of it should lead to a triangular intensity distribution with the tip at **som** = 0 and tip-height half of the unshaded intensity. The scan is performed by

> sscan som -2 2 81 2000 step-[scan of som from -2° to 2° ...

Most likely it was not correct and one gets a shifted tip position or even a plateau. One has to move there

```
> dr som <value>
```

```
> sp som 0 redefine the som zero
```

and repeat the `sty` scan. And so on with a higher resolution but with a reduced scan width, until `sty` is accurate within 0.05 mm.

4. The final step is to adjust the ω zero position using the reflected beam. The detector rotation is very accurate and has a defined zero-position. The detector is moved to an angle where still high reflectance can be assumed.

```
> dr stt 0.8
```

Then one has to scan ω

```
> sscan som 0 0.8 0.01 4000 step-scan of som
```

```
> peak analyse the last scan and find a peak
```

```
> center go to that peak
```

```
> sp som 0.4 set som to be 0.4° (half of the value of stt)
```

5. Eventually one has to repeat at least part of the procedure with narrower diaphragms. The final accuracy of ω should be better than 0.01° .

Now the sample is aligned and one can check if one really gets something like a reflectivity curve by performing a scan

```
> sscan som 0 2 stt 0 4 101 4000 step-scan of  $\omega$  from 0° to 2° and  
simultaneously of the detector from 0° to 4°
```

As a result one should see the direct beam around $\omega = 0$, the total reflection plateau, the decrease in intensity above ω^c and the oscillations.

The angular resolution is set with the diaphragm openings

```
> dah 1 0.8 2 the diaphragm apertures in horizontal direction  
are 1 mm, 0.8 mm, and 2 mm
```

Now the first real measurement can be performed:

```
> sscan som 0 2 stt 0 4 201 10000
```

Depending on the time available one can extend the ω -range, but with a somewhat longer counting time

```
> sscan som 2 4 stt 4 8 201 50000
```

After the measurements one has to remove the sample, and to drive the motors back to the initial positions upon adjustment.

3.4 data reduction

The measured curves are of the format I vs. ω . To get the reflectivity one has to transform ω into q_z , which is straight forward using eqn.23. The treatment for I is more complicated. For large (infinite) samples the complete beam hits the sample. Only the length of the *footprint* varies with ω . In this case for $\omega < \omega^c$ the total reflection plateau can be used for renormalisation to 1:

$$R(\omega) = I(\omega)/\hat{I} \quad (31)$$

with

$$\hat{I} = \frac{\int_{\omega=\omega_{\min}}^{\omega^c} I(\omega)}{\omega^c - \omega_{\min}} \quad (32)$$

The lower limit ω_{\min} is the start of the scan, or the lowest ω where the unreflected beam no longer hits the detector.

For small samples the situation changes: the footprint of the beam is larger than the sample (the beam width is wider than the projected sample width). The fraction of the incoming beam hitting the sample surface I' is proportional to $\sin \omega$ (for a parallel beam). Thus one has an additional correction:

$$I(\omega) = \frac{I'(\omega)}{\sin \omega} \quad (33)$$

to be applied prior to using eqns.31 and 32.

In the worst case one has a cross-over from the small to the large sample case. The corrections mentioned above assume a parallel beam - which is not the case. But due to the normalisation by \hat{I} the error introduced this way is quite small. The problematic consequence is, that there is no sharp ω where to switch from using eqn.33 to omitting it. To avoid this one normally aims for a small sample, always *bathed* in the beam.

The reflectivity obtained so far is still not the pure sample property, but contains the experimental resolution $f_{q_z}(q_z)$. I.e.

$$R'(q_z) = R(q_z) \otimes f_{q_z}(q_z) \quad (34)$$

The subscript q_z indicates that f varies with q_z . For the angle dispersive set-up the resolution is given by $\Delta\lambda/\lambda = \text{constant}$ and by $\Delta\omega$. If the latter one is also kept constant (by not changing the diaphragms during a scan) f does not vary with q_z and is often assumed to be a Gauß function.

Instead of de-convolution the measured curve with $f_{q_z}(q_z)$ it is more convenient to convolve the simulated data before the comparison of both. Often the resolution function is also a fit-parameter like thicknesses and densities.

The rapid decay of $R(q_z)$ with q_z has the consequence that the q_z range accessible is quite small. One limiting factor is the measuring time available: I scales with ω^{-4} so that for a sufficiently good statistics the counting time scales with ω^4 ! Even worse is the limit given by background. This might originate from the counter electronics, the neutrons scattered close to the sample (e.g. on the sample holder) or on the substrate (incoherent scattering), or just from the atmosphere. To illustrate the problem: If one wants to measure down to $R \approx 10^{-6}$ with an incoming intensity of 3000 cps one has to wait some 5 min for the one count from the surface!

For the comparison one normally assumes a constant background level and adds it to the simulated $R(q_z)$.

The simulations will be performed with the program Parratt32, running under Windows (sorry for that!). It is quite simple and of low flexibility, but its usage is intuitive. And the aim of this exercise is not to spend days in creating input files. Within Parratt32 the model parameters are entered in form of a table. It does all the calculations and finally plots the simulated $R(q_z)$ together with the measured curves. The fit should be done by eye (not by using the implemented fitting routine) by varying the parameters until the agreement is fine - or until one runs out of time.

3.5 protocol

During the experiment and the data reduction a logbook has to be kept. It should contain

- the names of the experimentalists and the date
- a short description of the planned experiment (not a copy of this manuscript: it does already exist!)
- a step-by-set description of all activities
 - manipulations
 - interpretations / justifications
 - commands given to the control software
- plots of
 - the raw data
 - the data after each reduction step
 - the data in comparison to the simulated curves
- a discussion of the results of the simulation (reliability, problems, options)
- an interpretation of the obtained density profiles